sensors

MDPI

Article

Research on Rainfall Monitoring Based on E-band Millimeter Wave Link in Nanjing Area

Siming Zheng [1,2], Congzheng Han [1,3,*], Juan Huo [1,3], Wenbing Cai [4], Yinhui Zhang [4], Peng Li [2], Gaoyuan Zhang [1,5], Baofeng Ji [1,5], Jiafeng Zhou[6]

1. Electronics and Communication Engineering Lab, Key Laboratory of Middle Atmosphere and Global Environment Observation, Institute of Atmospheric Physics, Chinese Academy of Sciences, Beijing 100029, China
2. School of Electronics and Information Engineering, Nanjing University of Information Science and Technology, Nanjing, 210044, China;
3. University of Chinese Academy of Sciences, Beijing 100049, China
4. Beijing Institute of Tracking and Telecommunications Technology, Beijing 100094, China
5. College of Information Engineering, Henan University of Science and Technology, Luoyang, 471023. China
6. Department of Electrical Engineering and Electronics, University of Liverpool, Liverpool, L69 3GJ, UK

* Correspondence: c.han@mail.iap.ac.cn;

Abstract: In recent years, the new technology of using commercial microwave links to measure precipitation has received more and more attention. Accurate rainfall observation data with high temporal and spatial resolution is essential for national disaster prevention and mitigation and climate response decisions. This paper introduces a field experiment of using an E-band millimeter wave link to obtain rain rate information in Nanjing area. The link is 3km long and operates at 71 GHz and 81 GHz. The post-processing of experimental data is crucial for accurate rainfall rate estimation. The difficulty in determining the attenuation baseline value is that the attenuation baseline is not constant over time. We first distinguish between the rainfall and the sunny periods, and then determine the classification threshold to determine the attenuation baseline in real time. We use the raindrop size distribution to calculate the rainfall rate and rainfall-induced attenuation, estimate and correct the influence of the wet antenna attenuation, and finally calculate the rainfall rate through the power law relationship between the rainfall rate and the rainfall-induced attenuation. The experimental results show that the correlation coefficient of the rainfall rate obtained from the inversion of the attenuation value of the E-band link in the 71 GHz band is about 0.90, and the mean square error is about 0.11 mm/h. It is about 0.91 in the 81 GHz band, and the mean square error is about 0.15 mm/h. By comparing with the rainfall rate measured by the laser raindrop spectrometer set up at the experimental site, we verified the reliability and accuracy of monitoring rainfall using the E-band millimeter wave link.

Keywords: electromagnetic wave propagation; E-band millimeter waves; rainfall induced attenuation; rainfall observation

1. Introduction

Precipitation plays an important role in our lives and is the source of life. It is an extremely important and active factor in the natural and social environment. The uneven distribution of precipitation in space and the instability of time change are the direct

causes of floods and droughts. Therefore, accurate real-time monitoring of precipitation is essential [1].

Traditional rain gauges do not have high spatial resolution due to the uneven distribution of the influences of complex terrain and dense buildings [2]. However, weather radars are easily affected by ground echoes at low elevation angles, and their measurement results are limited [3]. Studies have shown that millimeter waves are affected by many factors such as scattering, reflection, and atmospheric absorption in the process of space propagation. Among them, the influence of rainfall is the most obvious. The attenuation of the millimeter wave signal becomes greater with increasing frequencies [4-6]. Based on this feature, meteorological experts have proposed a method of using communication links to monitor rainfall and retrieve rainfall rate [7].

At present, many countries have carried out research on using the rain-induced attenuation characteristics of microwave links to retrieve precipitation, mainly in the frequency range of 15-40 GHz [8-11]. For example, in Israel, Messer et al. studied the estimation of rainfall rate by commercial microwave links, and analyzed various error sources that affect the estimation accuracy, including signal changes caused by antenna wetting and the uncertainty of the attenuation baseline [11-12]. Chwala et al. used the attenuation data of commercial microwave links in the high mountains of southern Germany, and used a method of detecting dry and wet periods through spectral time series analysis to estimate the near-surface rainfall rate [13]. In South Africa, Ahuna et al. evaluated the rainfall rate measurement of 10 locations in South Africa with a 5-minute integration time to obtain its cumulative distribution [14]. These studies have all contributed to the estimation of rainfall rate using microwave links, but they are all based on data collected from low-frequency links. With the rapid development of fifth-generation wireless communication technology (5G), more spectrum and wider bandwidth are required. However, the global bandwidth shortage has prompted the exploration of the underutilized millimeter-wave frequency band. Millimeter-wave has become one of the core technologies of 5G, and research on E-band link has gradually attracted attention recently [15-17]. Al-Samman et al. used a 1.8 km 73.5 GHz E-band link to analyze the rainfall rate and rainfall attenuation in tropical areas [18]. Luini et al. used two 325 m long links in the E-band (73 GHz and 83 GHz) to collect power data, identify rainfall events and eliminate wet antenna effects, and provide a higher-precision prediction model [19]. Their experiment also evaluated the accuracy of the statistical prediction model for terrestrial links currently recommended by the ITU-R in predicting rainfall induced attenuation along short-distance and high-frequency links in 5G networks.

In general, most of the published experimental studies are based on low-frequency link measurement data, and some are based on E-band link data collected in a few regions. However, there is not much research on rainfall rate retrieval based on E-band millimeter-wave links in China. Research experiments are needed to provide a highly accurate rain rate inversion model suitable for China. This article introduces an experiment for rainfall monitoring using data collected from an E-band millimeter wave link built in Nanjing, China. The structure is as follows. Section 2 introduces the system equipment used to build the E-band millimeter wave link, the auxiliary equipment for collecting rainfall data, and the propagation characteristics of the link. Section 3 introduces the method of processing the experimental data collected by the link, including wet-dry classification and real-time attenuation baseline calculation. Section 4 introduces the estimation method of the wet antenna effect, and finally obtains the attenuation value caused by rainfall to retrieve the rainfall rate. Section 5 presents the analysis and discussion of experimental results. Section 6 gives the conclusion.

2. Experimental equipment and link propagation characteristics

Figure 1(a) shows the E-band radio transceiver that we used. This device works in the frequency range of 71-76/81-86 GHz, adaptive modulation, and can directly configure local and remote devices through the network graphical user interface. Figure 1(b) shows the CLIMA laser precipitation monitor (also called raindrop spectrometer). The time resolution of the data recorded by this instrument is 1 minute, which is very suitable for measuring and detecting different types of precipitation, such as drizzle, rainfall, hail, snow, and mixed precipitation. The observed particles are divided into 22 diameter categories and 20 velocity categories. We can use this information to calculate the rainfall rate and the attenuation caused by rainfall.

(**a**) (**b**)

Figure 1. (**a**) E-band radio transceiver; (**b**) CLIMA laser precipitation monitor.

On a rainy day, the transmitted wireless signal is attenuated by raindrops due to scattering and absorption, which causes the signal level at the receiver to attenuate, so we can estimate the rainfall rate on the path. Figure 2 shows the E-band millimeter wave signal transmission structure.

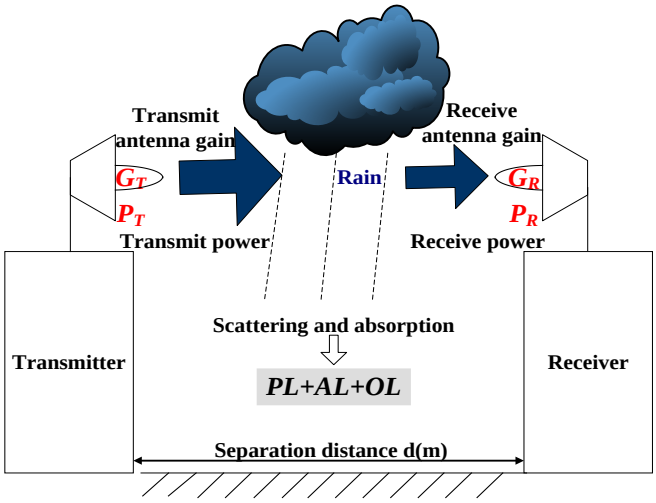

Figure 2. E-band millimeter-wave signal transmission structure.

The received power P_R (dB) can be expressed as:

$$P_R = P_T + G_T + G_R - PL - AL - OL \quad (1)$$

where P_R (dB) is the transmitted signal power, G_T (dBi), G_R (dBi) are the antenna gains of the transmitter and receiver, PL (dB) is the propagation path loss, AL (dB) is the atmospheric loss(5), and OL (dB) for other losses. PL can be expressed by the following formula [20]:

$$PL(f_c, d) = 32.4 + 20\log 10(f_c) + 10n\log 10(d/d_0) + \chi_\sigma, d \geq 1m \quad (2)$$

where f_c (GHz) is the carrier frequency, d is the distance between the transmitter and the receiver, the reference distance d_0 is 1m, and n is the path loss index. χ_σ is a zero-mean Gaussian random variable with σ standard deviation, and the unit is dB.

The attenuation model of AL is as follows:

$$AL = A_r + A_v + A_o + A_p \quad (3)$$

Atmospheric loss mainly includes the attenuation effects of dry air (including oxygen), humidity, fog, and rainfall. A_r (dB) is the attenuation caused by rainfall, A_v (dB) is the attenuation caused by water vapor, A_o (dB) is the attenuation caused by dry air, and A_p (dB) is the attenuation caused by non-rainfall, such as fog, rain, and snow.

Attenuation caused by rainfall A_r and equivalent path-averaged rainfall rate R (mm/h) have a power-law relationship. We can calculate the attenuation caused by rainfall through the simple formula provided in ITU-R P.838-3 [21]. The model is as follows:

$$A_r^{ITU-R} = \gamma_r^{ITU-R} l = kR^\alpha l \quad (4)$$

In the formula, γ_r^{ITU-R} is the rainfall induced attenuation, l is the link length, which is 3 km in this experiment, and k and α are the frequency compliance coefficients, which are related to the millimeter-wave operating frequency, rainfall temperature, polarization mode, and raindrop size distribution. In [21], the power-law coefficient corresponding to the 71 GHz link is [1.0409, 0.7193], and the power-law coefficient corresponding to the 81 GHz link is [1.1793, 0.7004]. Assuming that the rainfall rate is constant along this path, if we obtain the attenuation caused by rainfall, we can also calculate the rainfall rate based on this model. Next, we will introduce the steps and methods for obtaining the attenuation caused by rainfall from the link data.

3. Data processing

3.1. Preprocessing

We built an E-band millimeter wave link in Nanjing area and collected the received power data from December 2019 to March 2020, sampling every 1 minute with a resolution of 0.1 dB. First, the level signal received by the millimeter-wave link is processed. Due to the interruption of the data acquisition system, the original data shows missing values (Nan), and we will exclude the data with missing values. The total attenuation value on the link path is obtained by subtracting the transmit power from the received power. This link is a dual-polarization link, and only vertical polarization is used in this article. The raindrop spectrometer we use has a time resolution of 1 min for measuring rainfall rate, which is consistent with the time resolution of path attenuation. Figure 3(a) shows the signal strength P_R received by the E-band link on January 7, 2020. The frequencies are 71 GHz and 81 GHz, respectively. Figure 3(b) shows the rainfall rate R^{out} output by the raindrop spectrometer set up at the experimental site. It can be seen that after a rainfall

event occurs, the received signal intensity is attenuated accordingly, and the rainfall rate is positively correlated with the signal attenuation.

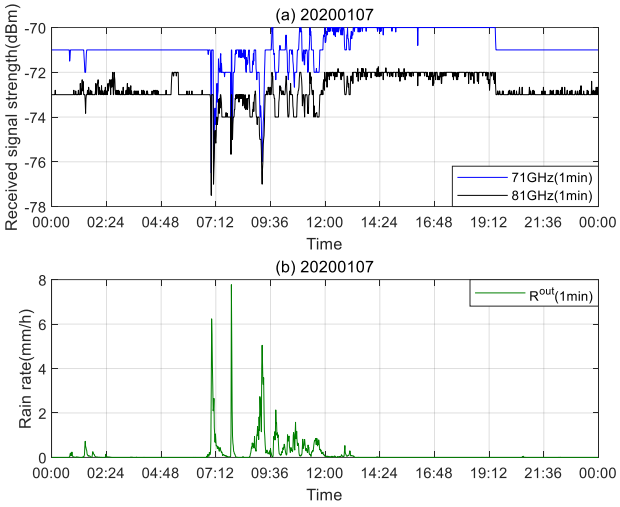

Figure 3. (**a**) The received signal intensity on January 7, 2020; (**b**) The rainfall rate output by the raindrop spectrum instrument.

3.2. Attenuation baseline calculation

From Figure 3(a), it can be observed that after the rainfall event ended (approximately at 12:00), P_R did not return to the signal strength during the drought period (before the rainfall event), but changed with time after the rainfall event. In the dry period of this day, when the frequency is 71 GHz, P_R fluctuates between -71 dBm and -70 dBm, and when the frequency is 81 GHz, P_R fluctuates between -73 dBm and -72 dBm. Therefore, the attenuation value during the drought period cannot be directly used as the baseline. We use the method in [22] to determine the attenuation baseline. Assuming that $A_T(t)$ is the total attenuation of the link over time, expressed here as:

$$A_T(t) = A_b(t) + A_r(t) \tag{5}$$

where $A_b(t)$ represents the attenuation baseline, and $A_r(t)$ represents the attenuation caused by rainfall. We define a moving window $W = [t-w, t]$ with a width of $w > 0$.

$$\bar{A}_{Wt} = \frac{1}{N_W} \sum_{k \in Wt} A(k) \tag{6}$$

$$S_{Wt}^2 = \frac{1}{N_W} \sum_{k \in Wt} \left(A(k) - \bar{A}_{Wt} \right)^2 \tag{7}$$

where N_W represents the number of measurements in W_t. The choice of window size has a great impact on wet and dry classification, and it should not be too large or too small. After weighing the results in this experiment, we choose $w = 25\ \text{min}$. According to the decision rule in [22], for a given threshold σ_0, $S_{Wt} > \sigma_0$, it means a rainy period; if $S_{Wt} \le \sigma_0$, it means a dry period.

The value of σ_0 is estimated from attenuation measurements collected during a dry period (usually 24 hours). Assuming that D represents a dry period and R represents a rainy period, the value of σ_0 is obtained by the following formula:

$$\sigma_0 = q_{85}\{S_{Wt} | t \in D\} \tag{8}$$

Among them, q_{85} denotes the 85% quantile, which is the threshold obtained after we analyzed the data of Nanjing from December 2019 to March 2020. When the window sizes w and σ_0 are determined, $A_b(t)$ can be determined according to the method in [22]:

$$A_b(t) = \begin{cases} \overline{A}_{Wt}, & t \in D \\ A_b(t-m), & t \in R \end{cases} \tag{9}$$

where m is the minimum value that makes $t-m \in D$. Let's take the attenuation on January 19, 2020 during the dry period as an example, and the calculated values of $\overline{A}_{Wt}$ and σ_0 are shown in Table 1:

Table 1. $\overline{A}_{Wt}$ and σ_0 obtained from the data on January 19, 2020.

Frequency	$\overline{A}_{Wt}$	σ_0
71GHz	67.8	0.03
81GHz	69.9	0.04

4. Rain rate inversion

4.1. Raindrop size distribution

For rainfall inversion, it is very necessary to find the rainfall rate and related attenuation of the actual rainfall event. We need to know the change of the raindrop size distribution (DSD) in the rainfall of a given intensity. We use the raindrop shape and size function to calculate the rainfall rate R^{DSD} (mm/h) [23], and use R^{DSD} to compare with the inverted rainfall rate in subsequent experiments. According to the DSD data of raindrops, the droplet density distribution is calculated as follows [24]:

$$N(D_i) = \sum_{j=1}^{20} \frac{N_{ij}}{V_j \times S \times T \times \Delta D_i} \left[m^{-3} \cdot mm^{-1}\right] \tag{10}$$

where N_{ij} represents the number of raindrops with a diameter at level i and speed at level j, and D_i is the diameter of raindrops at level i. S is the measurement area of the raindrop spectrometer, where the value of S is 0.0044. T is the sampling time of 60 s, ΔD_i is the diameter interval between two adjacent levels i and $(i+1)$, and V_j is the falling speed of the droplet with a speed of j.The rainfall rate R^{DSD} can be calculated using the formula proposed in [25]:

$$R^{DSD} = 6\pi \times 10^{-4} \sum_{i=1}^{22} \sum_{j=1}^{20} V_j \times D_i^3 \times N(D_i) \Delta D_i \left[mm/h\right] \tag{11}$$

Figure 4 shows the comparison between the output rainfall rate R^{out} of the raindrop spectrometer on January 7, 2020 and the rainfall rate R^{DSD} calculated by the raindrop DSD. Through observation, it can be seen that the output result of the raindrop spectrometer is higher than R^{DSD}, indicating that the actual rainfall rate and the instrument output rainfall

rate are different, so R^{DSD} is used as the reference rainfall rate in the subsequent experiments.

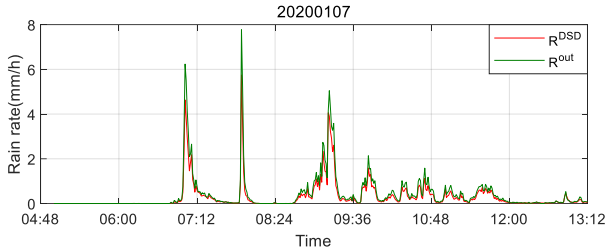

Figure 4. On January 7, 2020, the raindrop spectrum instrument output rain rate (green line) and raindrop DSD calculated rain rate (red line).

The raindrop shape and size function can be used to not only calculate the rainfall rate, but also express the specific attenuation γ (dB/km) [26]. Mie theory [27-28] is used to calculate the extinction coefficient of a single particle at millimeter-wave frequencies, expressed in integral form as follows:

$$\gamma_r^{DSD} = 4.343 \times 10^3 \int_D C_{\text{ext}}(D, f) N(D) dD \tag{12}$$

where $C_{ext}(D, f)$ is the Mie extinction cross-section with a droplet diameter of D, which depends on frequency and temperature. It characterizes the scattering and absorption characteristics of each raindrop at a given frequency f and polarization, and determines the attenuation caused by a single droplet. In addition to dimensional information, the application of Mie theory to calculate the extinction cross-section also requires a complex refractive index. Using the dielectric function of Liebe et al. [29], it covers the frequency range from 1 GHz to 1000 GHz.

The propagation experiment of Hansryd [30] et al. showed that compared with the low frequency band, the E-band millimeter-wave has a higher scattering efficiency for smaller raindrops and has a stronger dependence on DSD. The model provided in ITU-R P.838-3 shows that there is a power law relationship between the specific attenuation and the rainfall rate, therefore:

$$\gamma_r^{DSD} = k^{DSD} R^{DSD^{\alpha^{DSD}}} \tag{13}$$

This is a good approximation of the relationship between attenuation and rain rate. Our link length l is 3km, so the rainfall induced attenuation A_r^{DSD} calculated by DSD can be expressed as:

$$A_r^{DSD} = \gamma_r^{DSD} \times l = k^{DSD} R^{DSD^{\alpha^{DSD}}} l \tag{14}$$

Figure 5 is the first rainfall event that occurred in the 71 GHz band on January 7, 2020, comparing the three methods outlined above for estimating the rainfall induced attenuation. The blue line represents the rainfall induced attenuation after the link measurement data is processed by the method in Section 3, the red line is calculated from the measured DSD data, and the green line represents ITU-R P.838- 3. The proposed method is estimated. Comparing the corresponding rainfall induced attenuation in Figure 5, it can be seen that the trends of the three curves are similar. However, the attenuation A_r measured by the link is higher than the other two methods when the rain reaches the maximum as the rainfall event occurs, until the rainfall event ends. This deviation directly affects the accuracy of rainfall induced attenuation measured by link data. After excluding other effects, the wet antenna effect is the main reason for the difference between the measured

rainfall induced attenuation and the actual attenuation of the link [31]. We will study methods to eliminate this effect in the next section.

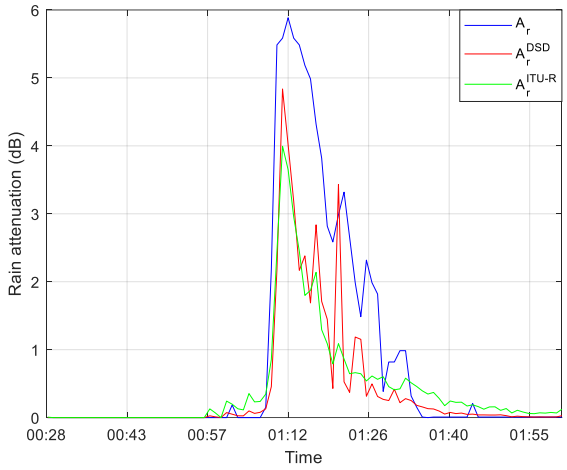

Figure 5. Rainfall induced attenuation at 71 GHz on January 7, 2020, blue line: predicted from link data, red line: estimated from DSD data, green line: using the method recommended by ITU-R P.838-3.

4.2. Wet Antenna Correction

When it rains, the water layer adheres to the surface of the reflector, radome, and horn cap. In this case it will cause significant signal attenuation [32-34]. Since they are almost vertical surfaces made of hydrophobic materials, the amount of water attached to the surface of the radome may have a maximum value, which will cause the attenuation caused by it to reach a saturated value.

An exponential relationship between the measured attenuation value A_r and the attenuation A_{wa} caused by the wet antenna is proposed in [35], as follows:

$$A_{wa} = C \cdot \left(1 - \exp\left(-d \cdot A_r\right)\right) \tag{15}$$

where C and d are model parameters. Tests have proved that the wet antenna attenuation increases with the lowest value of measured attenuation and rainfall rate, and finally it reaches the saturation value. In this case, C is selected as the representative of the largest difference between the forecast and the measurement observed in the time series. d is calculated by nonlinear regression of the model during the observation period [36].

It can be seen from Figure 6 that at 71 GHz, when A_r is 5.5 dB, A_{wa} reaches the saturation value mentioned in [28], so the wet antenna attenuation A_{wa} can be expressed as:

$$A_{wa} = \begin{cases} 2.5283\left(1 - e^{-0.3757A_r}\right), & A_r \le 5.5dB \\ 2.25, & A_r > 5.5dB \end{cases} \tag{16}$$

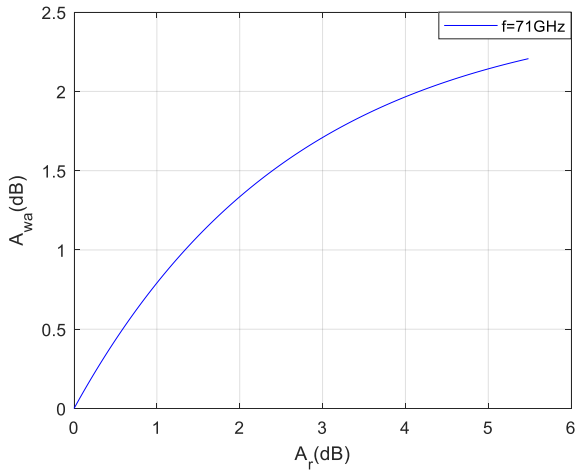

Figure 6. Curve fitting of A_r and A_{wa} at 71 GHz.

Similarly, as shown in Figure 7, at 81 GHz, when A_r is 4.5 dB, A_{wa} reaches a saturation value, so A_{wa} is expressed as follows:

$$A_{wa} = \begin{cases} 1.1270\left(1 - e^{-0.7265A_r}\right), & A_r \le 4.5dB \\ 1.1, & A_r > 4.5dB \end{cases} \quad (17)$$

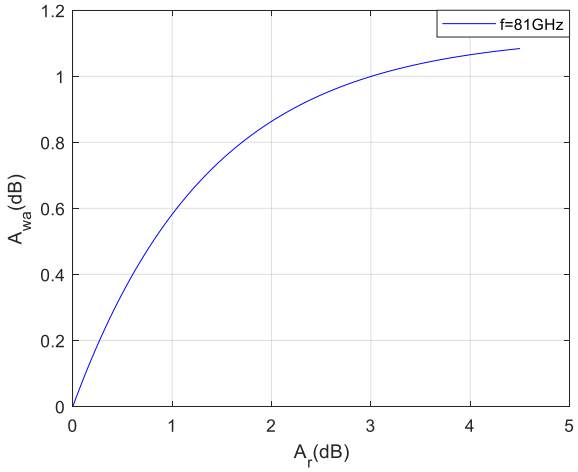

Figure 7. Curve fitting of A_r and A_{wa} at 81 GHz.

We apply the wet antenna correction model to the link data to predict rainfall-induced attenuation, and the corrected attenuation level A_r' can be obtained from $A_r' = A_r - A_{wa}$.

Figure 8 shows the first rainfall event that occurred in the 71 GHz band on January 7, 2020. The rainfall induced attenuation after correcting the influence of the wet antenna shows a better fitting effect than before the correction, and is closer to the result estimated from the DSD data and estimated using the ITU-R P.838-3 recommendation.

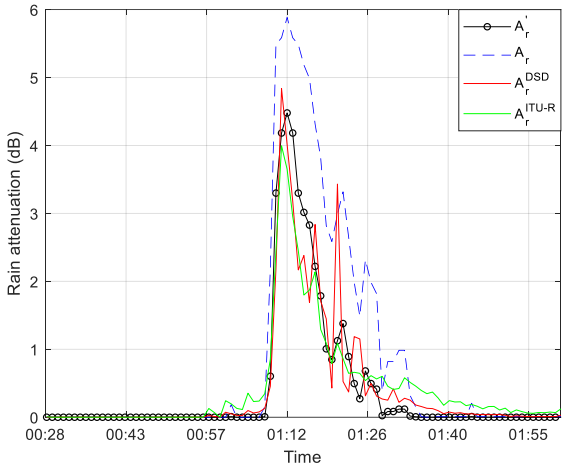

Figure 8. Rainfall induced attenuation at 71 GHz on January 7, 2020, black line: rainfall induced attenuation after correction, blue line: predicted from link data, red line: estimated from DSD data, green line: using the method recommended by ITU-R P.838-3.

4.3. Rain rate inversion result

We use the millimeter-wave link to collect data from December 2019 to March 2020 and analyze the rainfall events in these four months. We then apply the above model to invert the rainfall rate, and evaluate the inversion effect by calculating the Pearson correlation coefficient and the mean square error. The formula is as follows:

$$r\left(R_{M,i}, R_{D,i}\right) = r\left(X_i, Y_i\right) = \frac{1}{N-1}\sum_{i=1}^{N}\left(\frac{X_i - \mu_X}{\sigma_X}\right)\left(\frac{Y_i - \mu_Y}{\sigma_Y}\right) \quad (18)$$

$$MSE = \frac{1}{N}\sum_{i=1}^{N}\left(R_{M,i} - R_{D,i}\right)^2 \quad (19)$$

Among them, R_M represents the rainfall rate estimated by the link data, and R_D represents the rainfall rate calculated by the DSD and the raindrop spectrum instrument measured the rainfall rate. μ_X and σ_X are the mean and standard deviation of $X_i = R_M$, and μ_Y and σ_Y are the mean and standard deviation of $Y_i = R_D$. The higher the correlation coefficient and the smaller the mean square error. It means that there is better similarity between the two data sets, indicating that the rainfall rate estimation from the millimeter-wave link is closer to the true rain rate. Figure 9 shows the received signal strength and rainfall rate results. Table 2 lists the 6-day rainfall rate correlation coefficient and mean square error value.

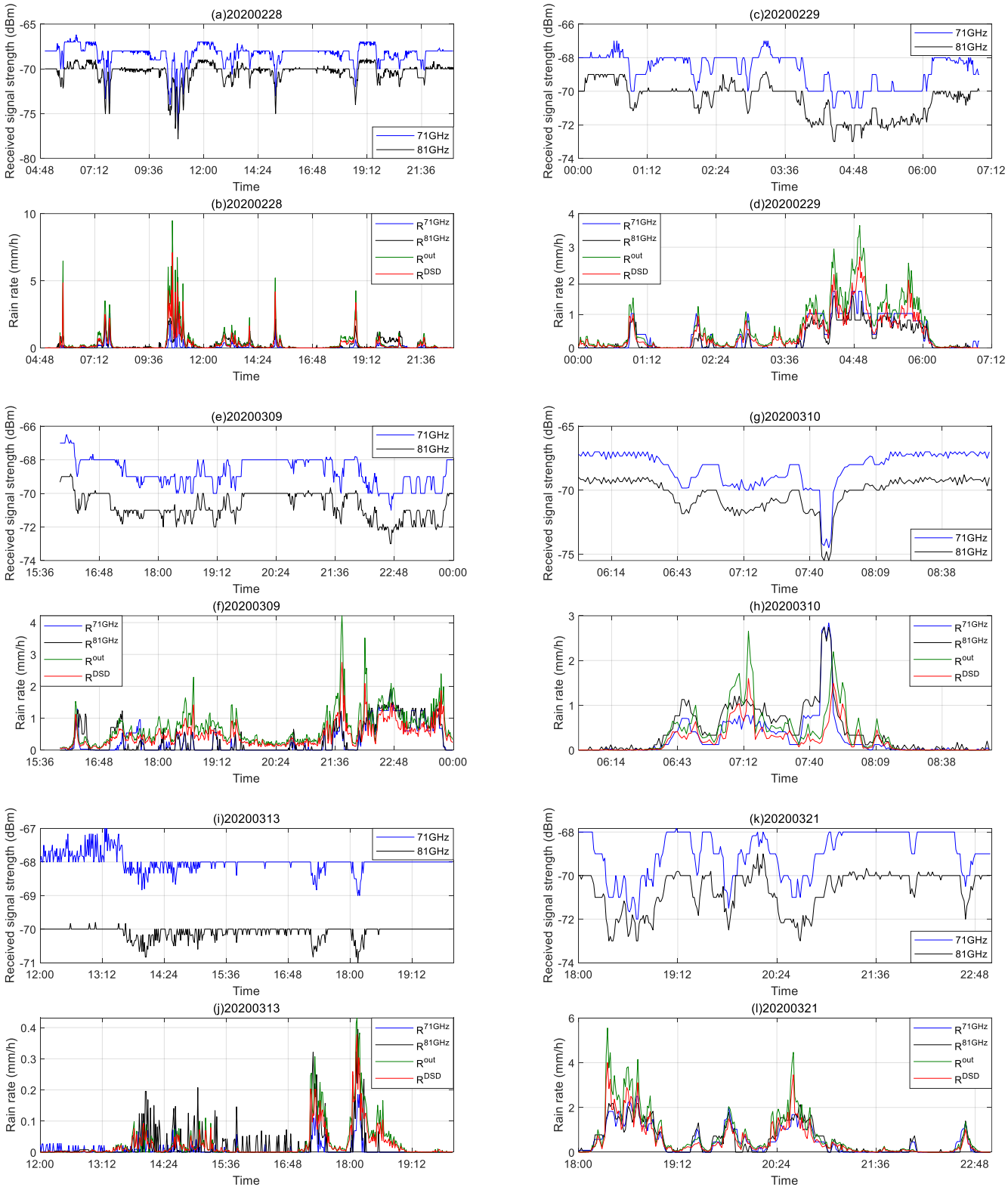

Figure 9. The received signal strength P_r of 71 GHz and 81 GHz on different days. The comparison result of link retrieved rainfall rate R^{71GHz} and R^{81GHz}, raindrop spectrometer output rain rate R^{out} and DSD data to calculate rainfall rate R^{DSD}.

Table 2. Correlation and mean square error of the estimated rainfall rate (based on the 71 GHz and 81 GHz link) and rainfall rate recorded by disdrometer

Date	Frequency	R^{out}		R^{DSD}	
		r (-)	MSE (mm/h)	r (-)	MSE (mm/h)
2020/02/28	71GHz	0.90	0.11	0.89	0.10
	81GHz	0.91	0.15	0.89	0.06
2020/02/29	71GHz	0.88	0.19	0.86	0.33
	81GHz	0.89	0.22	0.87	0.07
2020/03/09	71GHz	0.59	0.37	0.61	0.16
	81GHz	0.57	0.36	0.60	0.17
2020/03/10	71GHz	0.55	0.22	0.53	0.17
	81GHz	0.67	0.18	0.65	0.21
2020/03/13	71GHz	0.59	0.01	0.61	0.01
	81GHz	0.63	0.01	0.63	0.01
2020/03/21	71GHz	0.87	0.36	0.87	0.13
	81GHz	0.84	0.37	0.84	0.16

5. Discussion

From the experimental results, the accuracy of the rainfall rate retrieved from millimeter-wave link data is relatively high. As shown in Table 2, about 73% of the correlations are above 0.6, and 95% of the mean square errors are less than 0.5 mm/h, which shows that the millimeter-wave link in the E-band can monitor rainfall well. Figure 9 shows the received signal strength and rainfall strength of the day. It can be seen that as the rainfall event occurs, the signal strength is attenuated accordingly. The R^{71GHz} and R^{81GHz} shown in the figure are the results of eliminating the wet antenna effect. It can be seen from the comparison results of link retrieved rainfall rate with R^{out} and R^{DSD} that the retrieved rainfall rate is lower when the rainfall is heavy. This may be related to the excessive elimination of attenuation when removing the effect of the wet antenna, which means that part of the attenuation caused by the wet antenna will be eliminated when the above method correctly extracts the rainfall induced attenuation, which is consistent with the conclusions in the previous study [19]. The estimation process is relatively insensitive to the attenuation of the wet antenna that occurs on a long link because the attenuation along its path is greater than the attenuation of the wet antenna. In addition, it can be seen from the figure, under the same conditions, compared with the 71 GHz millimeter-wave link, the 81 GHz millimeter-wave has a larger attenuation, and the estimated rainfall rate is slightly higher than the rainfall rate estimation based on the 71 GHz link, which indicates that the 81 GHz link provides better estimation accuracy for rainfall monitoring. In addition, it can be seen from the figure that, under the same conditions, the signal attenuation of 81 GHz millimeter-wave is larger than that of 71 GHz millimeter-wave link. Moreover, the rainfall rate retrieval result is also slightly higher than the 71 GHz result, indicating that the millimeter-wave link in the high frequency band is preferrable for monitoring

rainfall. From Table 2 we can also see that the mean square error of R^{71GHz}, R^{81GHz} and R^{DSD} is about 0.01-0.35 mm/h lower than the mean square error of R^{out}, and this difference is relatively small. This shows that the difference between R^{out} and R^{DSD} will not have a great impact on the results of rainfall retrieval. But in order to retrieve rainfall more accurately, this cannot be easily ignored.

Taking the rainfall event on February 29, 2020 as an example, it can be determined from the data of R^{out} and R^{DSD} in Figure 9(d) that there has been some drizzle since 00:00 on this day. We found that for small rainfall, the received signal strength of millimeter-wave has small fluctuations, which can be seen from Figure 9(c). But this is a fluctuation lower than the attenuation baseline, and the inverted rainfall is not reflected. From the 81 GHz signal receiving strength in the figure, it can be seen that the small fluctuations from 00:00 to 01:00 are higher than the attenuation baseline, which is also reflected in the rainfall inversion results. It shows that the high-frequency link is more suitable for light rain monitoring. On the other hand, this may be related to the size of the time window selected in Section 3.2, which affects the determination of the attenuation baseline. If a small one is chosen, this attenuation will be reflected. But the disadvantage of this is that it will overestimate the rainfall attenuation, thereby reducing the accuracy of rainfall retrieval. The improved correlation and lower mean square error in Table 2 indicate that the window size we choose is appropriate, which also shows that this rainfall retrieval model is accurate and effective.

6. Conclusions

This article introduces the research results of the E-band millimeter-wave link built in Nanjing, located in Southern China. Signals at E-band experience greater attenuation by rainfall. It is relatively easy to measure. We use a 3 km long link, so the link's ability to accurately quantify the rainfall rate during light rainfall is stronger than that of the traditional microwave links operating at 15-40 GHz. The measurement data is collected with a high time resolution at 1 min sampling interval.

The experimental results show that the method of separating rainfall induced attenuation and eliminating wet antenna attenuation studied in the low frequency band is also applicable to the E frequency band. We are doing research on rainfall events with a rain rate of about 0-4 mm/h. The correlation between the retrieved rainfall rate and the rainfall rate measured by the raindrop spectrometer at 71 GHz is about 0.9, with a mean square error of about 0.11 mm/h. The correlation at 81 GHz is about 0.91, with a mean square error of about 0.15 mm/h. This further confirms the high sensitivity of the E-band millimeter-wave link to light rainfall. The determination of the attenuation baseline is very important for accurately separating the rainfall induced attenuation. This article uses a simple wet and dry classification and then determines the baseline method. Compared with the model provided by ITU-R P.838-3 and the attenuation calculated by DSD data, the rainfall induced attenuation estimated by this method is closer to the calculation result of DSD data, indicating that this method is accurate and effective. In our research, the attenuation caused by the wet antenna is estimated through DSD data and an effective model. The attenuation caused by the wet antenna in a rainfall event is about 2 dB, which is a relatively small value, indicating that the impact of the wet antenna attenuation on the rainfall rate retrieval in the E-band is less than the low frequency band of 15-40 GHz. For a long E-band millimeter wave link, since we cannot always assume that the rainfall rate along its path is uniformly distributed, this may cause some errors, which is also a factor that affects the experimental results. In a sufficiently long link, it is also possible to separate the attenuation caused by water vapor, which of course is challenging in practice.

Author Contributions: Conceptualization, SM.Z. and CZ.H.; methodology, SM.Z.; software, SM.Z.; validation, SM.Z., CZ.H. and P.L.; formal analysis, CZ.H.; investigation, SM.Z.; resources, CZ.H.,

GY.Z., and BF.J, JF.Z.; data curation, J.H; writing—original draft preparation, SM.Z.; writing—review and editing, SM.Z, J.H.; visualization, SM.Z.; supervision, P.L.; project administration, WB. C and YH. Z.; funding acquisition, CZ.H. All authors have read and agreed to the published version of the manuscript.

Funding: This research received no external funding

Acknowledgments: The author would like to thank Xichuan Liu and Pu Kang for conducting the millimeter-wave measurement and sharing the data for this study. The authors thanks anonymous reviewers for providing helpful advice.

This work was financially supported in part by the National Natural Science Foundation of China (Grant No. 41605122, 41775032, 61701172, 61801170); LAGEO of Institute of Atmospheric Physics, Chinese Academy of Sciences (LAGEO 2019-2); Young Backbone Teachers in Henan Province (2018GGJS049); Henan Province Young Talent Lift Project (2020HYTP009); Program for Science & Technology Innovation Talents in the University of Henan Province (20HASTIT022). China Postdoctoral Science Foundation (2018M633351), Wuxi Guo Ke Chao Qing Neng Technology Co., Ltd.

Conflicts of Interest: The authors declare no conflict of interest.

References

1. Hou, A.Y.; Kakar, R.K.; Neeck, S.; Azarbarzin, A.A.; Kummerow, C.D.; Kojima, M.; Oki, R.; Nakamura, K.;Iguchi, T. The global precipitation measurement mission. Bull. Am. Meteorol. Soc 2014, 95, 701-722.
2. Sevruk, B. Rainfall measurement: gauges, in: encyclopedia of hydrological sciences, edited by: Anderson, M. G. and Mc-Donnell, J. J., John Wiley & Sons, Ltd, Chichester 2005, https://doi.org/10.1002/0470848944.hsa038.
3. Berne, A.; Krajewski.; W, F. Radar for hydrology: Unful-filled promise or unrecognized potential. Adv. Water Resour 2013, 51, 357-366, https://doi.org/10.1016/j.advwatres.2012.05.005.
4. Rappaport, T. S.; Heath, R. W.; Jr, R. C.; Daniels.; Murdock, J. N. Millimeter wave wireless communications. London, U.K.: Pearson,2014.
5. Han, C.; Duan, S. Impact of atmospheric parameters on the propagated signal power of millimeter-wave bands based on real measurement data, in IEEE Access 2019, 7, 113626-113641, doi: 10.1109/ACCESS.2019.2933025.
6. Rappaport, T. S. Millimeter wave mobile communications for 5G cellular: it will work!. in IEEE Access 2013, 1, 335-349, doi: 10.1109/ACCESS.2013.2260813.
7. Messer, H. A.; Zinevich.; Alpert, P. Environmental monitoring by wireless communication networks. Science 2006, 312-713.
8. Imhoff, R. O.; Overeem, A.; Brauer, C. C.; Leijnse, H.; Weerts, A. H.; Uijlenhoet, R. Rainfall nowcasting using commercial microwave links. Geophysical Research Letters 2020, 47, GL089365, https://doi.org/10.1029/2020GL089365.
9. Han, C.; Bi, Y.; Duan, S.; Lu, G. Rain rate retrieval test from 25-GHz, 28-GHz, and 38-GHz millimeter-wave link measurement in Beijing. in IEEE Journal of Selected Topics in Applied Earth Observations and Remote Sensing 2019, 12(8), 2835-2847, doi: 10.1109/JSTARS.2019.2918507.
10. Graf, M.; Chwala, C.; Polz, J.; Kunstmann, H. Rainfall estimation from a German-wide commercial microwave link network:Optimized processing and validation for 1 year of data. Hydrology and Earth System Sciences 2020, 24(6), 2931-2950, https://doi.org/10.5194/hess-24-2931-2020.
11. Zinevich, A.; Messer, H.; Alpert, P. Prediction of rainfall intensity measurement errors using commercial microwave communication links. Atmos. Meas. Tech 2010, 3(5), 1385-1402.
12. Messer, H.; Zinevich, A.; Alpert, P. Environmental sensor networks using existing wireless communication systems for rainfall and wind velocity measurements. IEEE Instrum. Meas.Mag 2012, 15(2), 32-38.
13. Chwala, C.; Gmeiner, A.; Qiu, W.; Hipp, S.; Nienaber, D.; Siart, U. Precipitation observation using microwave backhaul links in the alpine and pre-alpine region of Southern Germany. Hydrology and Earth System Sciences 2012, 16(8), 2647-2661, https://doi.org/10.5194/hess-16-2647-2012.
14. Ahuna, L.N.; Afullo, T.J.; Alonge, A.A. 30-second and one-minute rainfall rate modelling and conversion for millimetric wave propagation in south africa. in SAIEE Africa Research Journal 2016, 107(1), 17-29, doi: 10.23919/SAIEE.2016.8532248.

15. Ostrometzky, J.; Raich, R.; Bao, L.; Hansryd, J.; Messer, H. The wet-antenna effect—a factor to be considered in future communication networks. in IEEE Transactions on Antennas and Propagation 2018, 66(1), 315-322, doi: 10.1109/TAP.2017.2767620.
16. Han, C.Z.; Huo, J.; Gao, Q.Q.; Su, G.Y.; Wang, H. Rainfall monitoring based on next-generation millimeter-wave backhaul technologies in a dense urban environment. Remote Sensing 2020, 12, 1045, 10.3390/rs12061045.
17. Pu, K.; Liu, X.; He, H. Wet antenna attenuation model of E-band microwave links based on the LSTM Algorithm. in IEEE Antennas and Wireless Propagation Letters 2020, 19(9), 1586-1590, doi: 10.1109/LAWP.2020.3011463.
18. Al-Samman, A.M.; Mohamed, M.; Ai,Y.; Cheffena, M.; Azmi, M. H.; Rahman, T. A. Rain attenuation measurements and analysis at 73 GHz E-band link in tropical region. in IEEE Communications Letters 2020, 24(7), 1368-1372, doi: 10.1109/LCOMM.2020.2983361.
19. Luini, L.; Roveda, G.; Zaffaroni, M.; Costa, M.; Riva, C.G. The impact of rain on short E-band radio links for 5G mobile systems: experimental results and prediction models. in IEEE Transactions on Antennas and Propagation 2020, 68(4), 3124-3134, doi: 10.1109/TAP.2019.2957116.
20. Daniels, R.C.; Heath, R.W.; Murdock, J. N.; Rappaport, T. S. Millime-ter wave wireless communications: systems and circuits. Upper Saddle River, NJ, USA: Prentice Hall 2014.
21. Specific attenuation model for rain for use in prediction methods, ITU-R document P .838-3, Switzerland, 2005.
22. Schleiss, M.; Berne, A. Identification of dry and rainy periods using telecommunication microwave links. IEEE Geosci. Remote Sens. Lett 2010, 7(3), 611-615.
23. Lam, H.Y.; Luini, L.; Din, J.; Capsoni, C.; Panagopoulos, A.D. Investigation of rain attenuation in equatorial Kuala Lumpur. IEEE Antennas Wireless Propag. Lett 2012, 11, 1002-1005.
24. Marshall, J. S.; Palmer, W. M. The distribution of raindrops with size. J. Atmos. Sci 1948, 5(4), 165-166.
25. Chwala, C.; Kunstmann, H. Commercial microwave link networks for rainfall observation: Assessment of the current status and future challenges. Wiley Interdiscipl. Rev., Water 2019, 6(2), e1337.
26. Lam, H.Y.; Luini, L.; Din, J.; Capsoni, C.; Panagopoulos, A.D. nvestigation of rain attenuation in equatorial Kuala Lumpur. IEEE Antennas Wireless Propag. Lett 2012, 11, 1002-1005.
27. Mie, G. Beiträge zur Optik trüber Medien, speziell kolloidaler Metal-lösungen. Ann. Phy 1908, 25, 377-445.
28. Bohren, C. F.; Huffman, D. R. Absorption and scattering of light by small particles. New York: Wiley 1998.
29. Liebe, H.J.; Hufford, G.A.;Cotton, M.G. Propagation modeling of moist air and suspended water/ice particles at frequencies below 1000GHz. in AGARD Conf. Proc. 542, Atmos. Propag. Effects Natural Man-Made Obscurants Visible MM-Wave Radiat 1993, 3.1-3.10.
30. Hansryd, J.; Li, Y.; Chen, J.; Ligander, P. Long term path attenuation measurement of the 71-76 GHz band in a 70/80 GHz microwave link. in Proceedings of the Fourth European Conference on Antennas and Propagation 2010,1-4.
31. Crane, R.K. Analysis of the effects of water on the ACTS propagation terminal antenna. IEEE Trans. Antennas Propag 2002, 50(7), 954-965.
32. Jacobson, M.D.; Hogg, D.C.; Snider, J.B. Wet reflectors in mil-limeter-wave radiometry-experiment and theory. IEEE Trans. Geosci.Remote Sens 1986, GRS-24(5), 784-791.
33. Islam, M.; Tharek, A.; Din J.; Chebil, J. Measurement of wet an-tenna effects on microwave propagation-an analytical approach. in Proc. Asia-Pacific Microw. Conf , 1547-1551.
34. Minda, H.; Nakamura, K. High temporal resolution path-average rain gauge with 50-GHz band microwave. J. Atmos. Ocean. Technol 2005, 22(2), 165-179.
35. Kharadly, M.M.Z.; Ross, R. Effect of wet antenna attenuation on propagation data statistics. IEEE Trans. Antennas Propag vol. 2001, 49(8), 1183-1191.
36. Garcia-Rubia, J.M.; Riera, J. M.; Garcia-del-Pino, P.; Bernarroch, A. Attenuation measurements and propagation modeling in the W-band. IEEE Trans. Antennas Propag 2013,61(4), 1860-1867.

37. Fencl, M.; Dohnal, M.; Valtr, P.; Grabner, M.; Bareš, V. Atmospheric observations with E-band microwave links-challenges and opportunities. Atmos.Meas.Tech.Discuss 2020, https://doi.org/10.5194/amt-2020-28, in review, 2020. 452 453